Provisional chapter

Inorganic Nanostructures Decorated Graphene

Hong Ngee Lim, Nay Ming Huang,
Chin Hua Chia and Ian Harrison

Additional information is available at the end of the chapter

1. Introduction

1.1. Why use graphene for the assembly of nanostructures?

Graphene, with zero energy gap between the highest occupied molecular orbit and the lowest unoccupied molecular orbit (HOMO-LUMO), offers a unique two-dimensional (2-D) environment for fast electron transport and has potential applications in electronic devices [1, 2]. Other consequences of the band structure is the opacity which is wavelength independent [3], and thermal conductivity [4]. The four edges of a graphene sheet provide significant number of centres for fast heterogeneous electron transfer [1], when compared to single-walled carbon nanotubes (SWCNTs) for which heterogeneous electron transfer occurs only at the two ends of the nanotube [5]. Consequently, graphene sheets may have wider applicability in electrochemistry [6]. While graphite is brittle, graphene's flexibility is beneficial for use in electromechanical devices [7] and energy storage devices [8]. In the energy storage devices, its weight is of extremely important and the specific area per unit weight is an important figure of merit. Graphene exhibits a theoretical surface area of 2630 $m^2 g^{-1}$, which is ~ 260 times greater than graphite and twice that of CNTs [9]. Thus, graphene provides a way of enhancing the electrochemical catalytic activity of materials by greatly increasing the high surface area [10]. The intriguing electronic, optical, electrochemical, mechanical and thermal properties of graphene make it an indispensable material in various kinds of synthesis processes.

Various inorganic nanostructures have been prepared over the last two decades due to the special properties of nanostructured materials. Previously, 2-D ZnO nanoplates [11], 1-D PbS nanorods [12], 0-D semiconductor materials [13] and core-shell magnetic nanoparticles have been produced [14]. However, heavy aggregation of the nanostructures, resulted by van der Waals forces between the particles, may limit their special properties and cause structural instability, thus reduce their applicability. To prevent this clustering from occurring, nanocomposites, consisting of the nanoparticles embedded within a matrix compound, can be used.

These nanocomposites preserve the unique properties of the nanoparticles whilst often having the additional performance benefits of the matrix compound itself.

With large surface area and the unique properties given above, graphene is an attractive choice as the matrix for inorganic nanostructures [15]. Functionalization of graphene sheets with various nanostructures can further enhance the properties of graphene. Heterostructures consisting of nanostructures distributed on the surface of graphene could potentially display not only the unique properties of nanostructures [16] and those of graphene [2, 17, 18], but also additional novel functionalities and properties due to the interaction between them. Moreover, the growth of the nanostructures can take place easily when graphene is used as a matrix due to the planar structure of graphene, in comparison to the hollow tubal-shaped CNTs. The particle size and size distribution of nanostructures are small and narrow when graphene is used as a support for the growth of nanostructures [19-21].

2. Inorganic nanostructures decorated graphene

Graphene nanocomposites can be made from graphene oxide (GO) which is essentially a graphene sheet containing oxy-functional groups, such as epoxy, hydroxyl, carbonyl, and carboxylic, on the surface. The reactive functional groups provide a means of attaching the nanoparticles to the graphene sheet [22, 23]. The GO starting material can be simply and economically synthesized using chemical oxidation of graphite [24]. Graphene manufactured using this highly scalable synthesis route is also popularly known as reduced GO (rGO). Using GO as a support for metallic ions, many types of different nanocomposites have been made. The overview of the types of materials and synthesis methods pertaining to the graphene-based nanostructures are presented in Table 1 along with the potential application for the nanocomposites.

Inorganic Nanostructure	Morphology and Dimension	Synthesis Method	Potential Application	Reference
Metal				
Ag	16.9±3.5 nm	Rapid thermal treatment	Antibacterial agent, nanofluids for cooling technology, water treatments, surface-enhanced Raman scattering (SERS), transparent and conductive film, electrochemical immunosensor, and catalysis	[25]
Ag	~420 nm	Laser assisted photocatalytic reduction	Solar energy conversion	[26]
AgAu	50–200 nm	In situ chemical synthesis	Electrochemical immunosensing	[27]
Au	30-70 nm	Laser assisted photocatalytic reduction	Solar energy conversion	[26]

Inorganic Nanostructure	Morphology and Dimension	Synthesis Method	Potential Application	Reference
Au	30 nm	Cyclic voltammetry scanning	Detection of mercury	[28]
Ni	Single-layered	Electroless Ni-plating	Electrodes, sensors, hydrogen-storage, production of fuel cell	[29]
Pd	13±2 nm	Electrochemical codeposition	An anode catalyst for formic acid electrooxidation	[30]
Pd	5–7 nm	Laser irradiation	CO oxidation	[31]
Pt	5–7 nm	Laser irradiation	CO oxidation	[31]
PtRu	2 nm	Microwave	Electrocatalysts for methanol oxidation	[32]
Metal oxide				
Ag_2O	45 nm	In situ oxidation route	Supercapacitor	[33]
CoO	5–7 nm	Laser irradiation	CO oxidation	[31]
CuO	< 20 nm	In situ chemical synthesis	Glucose biosensor	[34]
CuO	30 nm	Hydrothermal	Anode for lithium-ion batteries	[21]
Fe_3O_4	20, 30 and 40 nm	In situ chemical synthesis	Sensors, supercapacitors, drug delivery systems, waste water treatment	[20]
Fe_3O_4	12.5 nm	Gas/liquid interface reaction	Anode for lithium-ion batteries	[35]
Mn_3O_4	10 nm	Ultrasonication	Supercapacitors	[36]
NiO	32 nm	Hydrothermal	Anode for lithium-ion batteries	[37]
PbO	image not shown	Electrochemical route	Detection of trace arsenic	[38]
SnO_2	10 nm	Microwave	Detection of mercury(II)	[19]
SnO_2	4-5 nm	One-step wet chemical method	Detection of cadmium(II), lead(II), copper(II), and mercury(II)	[39]
SnO_2	2–3 nm	Microwave	Supercapacitor	[32]
SnO_2	4–5 nm	Microwave autoclave	Anode for lithium-ion batteries	[40]
SnO_2	2–6 nm	Gas/liquid interface reaction	Anode for lithium-ion batteries	[41]
SnO_2	4–6 nm	In situ chemical synthesis	Anode for lithium-ion batteries	[42]
TiO_2	~20 nm	Hydrothermal	Detection of mercury	[43]
TiO_2	4–5 nm	Sonochemical	Photocatalyst	[44]
TiO_2 (P25)	~30 nm	Hydrothermal	Photocatalyst	[45]
TiO_2 (P25)	~30 nm	Hydrothermal	Photoelectrocatalytic degradation	[46]
ZnO	nanorods, an approximated diameter of ~90 nm and length of ~3 μm	Hydrothermal	Solar cells, gas sensors, transparent conductors, catalysis	[47]

Inorganic Nanostructure	Morphology and Dimension	Synthesis Method	Potential Application	Reference
ZrO_2	~42 nm	Electrochemical route	Enzymeless methyl parathion sensor	[48]
Metal oxides				
Bi_2WO_6	nanoparticles containing square nanoplates, 100–300 nm	Reflux	Photocatalyst	[49]
$La_2Ti_2O_7$	nanosheets, comprehensively integrated	Expansion and UV irradiation	Photocatalyst	[50]
$NiFe_2O_4$	6.5 nm	Hydrothermal	Anode for lithium-ion batteries	[51]
Pd-CoO	5–7 nm	Laser irradiation	CO oxidation	[31]
Others				
Ag/TiO_2	TiO_2 layer coexists with Ag	Dipping-lifting in sol-gel solution, reducing process and interface reaction	Photoelectrochemical conversion	[52]
CdS	7.5–20 nm	Solvothermal	Photocatalyst	[53]
Core-shell $Fe@Fe_2O_3$@ Si-S-O	mean of 22 nm	One-pot thermodecomposition	Chromium removal	[54]
Fe_2O_3-ZnO	Fe_2O_3 ~50 nm, ZnO <10 nm	Hydrothermal	Photocatalyst	[55]
FeS_2	spherical, ~50 nm	Hydrothermal	Solar energy conversion	[56]
SnSb	quasi-spherical, 30–40 nm	Solvothermal	Anode for lithium-ion batteries	[57]

Table 1. A summary of inorganic nanostructures decorated graphene and their potential applications. (Note: If the inorganic nanostructures are nanoparticles, the shape is not mentioned under the column of Morphology and Dimension.)

3. Interaction of nanostructures with graphene

The widely accepted mechanism for the synthesis of inorganic nanostructures decorated graphene is the attraction of the positively-charged metal ions by the polarised bonds of the functional groups on the GO. The attachment of the metal ions to the surface and edges of the GO results in a redox reaction and the formation of nucleation sites, which eventually leads to the growth of nanostructures on the 2-D graphene sheets. An example of this process is the redox hybridization process which occurs between GO and Fe^{2+} to form Fe_3O_4/rGO nanocomposite and this is shown in Figure 1 [58]. The Fe^{2+} ions are first attached to the surface by the functional groups on the surface of the GO sheets (Figure 1a). The GO acts as an oxidizing

agent (Equation 1), effectively increasing the oxidation state of the Fe ions from Fe^{2+} to Fe^{3+}. This is followed by the reaction of the Fe^{3+} ions, in an alkaline condition, into Fe_3O_4 nanoparticles (Equation 2) on the surface of the rGO. The complete stoichiometry is depicted by Equation 3. During the redox reaction, the polar oxygenated functional groups on the GO sheets serve as the anchoring sites for the Fe_3O_4 nanoparticles, consequently preventing serious agglomeration of the magnetic nanoparticles (Figure 1b).

$$2Fe^{2+} + GO \rightarrow 2Fe^{3+} + rGO \tag{1}$$

$$Fe^{2+} + 2Fe^{3+} + 8OH^- \rightarrow Fe_3O_4 + 4H_2O \tag{2}$$

$$3Fe^{2+} + GO\left(8OH^-\right) \rightarrow Fe_3O_4 + 4H_2O + rGO \tag{3}$$

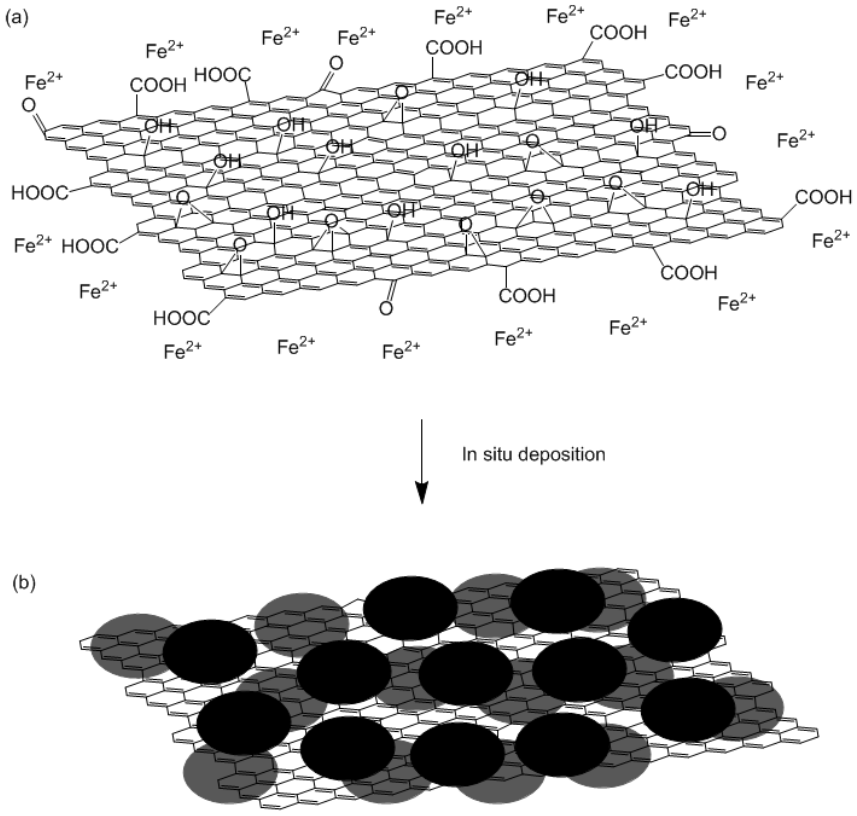

Figure 1. Schematic illustration of the formation of Fe_3O_4/rGO nanocomposite via a one-step in situ chemical deposition method [20].

In the case of metal/graphene, the nanocomposites are produced through simultaneous reduction of GO and metal ions [29, 31, 32]. In the absence of a reducing environment as in pure water but under the illumination of a radiating energy such as laser, the reduction mechanism of the metal ions (M^{2+}) involving the photogenerated electrons from GO are shown by Equations 4–7, where GO is partially reduced as portrayed by Equations 6 and 7 [26].

$$GO + h\nu \rightarrow GO\left(h^{+} + e^{-}\right) \tag{4}$$

$$4h^{+} + 2H_2O \rightarrow O_2 + 4H^{+} \tag{5}$$

$$M^{+} + GO\left(e^{-}\right) \rightarrow GO + M \tag{6}$$

$$GO + 4e^{-} + 4H^{+} \rightarrow rGO + 2H_2O \tag{7}$$

In the presence of a reducing agent such as sodium borohydride, $NaBH_4$ used for the synthesis of Ni/graphene, Ni ions and the COOH groups on the surface of the GO sheets were reduced to Ni metal and CH_2OH, respectively. The corresponding equation may proceed as represented by Equation 8 [29].

$$4Ni_2^{2+} + BH_4^{-} + 8OH^{-} \rightarrow 4Ni + BO_2^{-} + 6H_2O, -COOH \xrightarrow{[BH_4^{-}]} -CH_2OH \tag{8}$$

The incorporation of nanoparticles could be through chemisorption, physisorption, electrostatic interaction, van der Waals or covalent bonding with rGO [21, 22]. The attachment of nanostructures onto the surface of the graphene reduces the attractive interactions between the rGO sheets and, minimizes the aggregation and restacking of rGO during the reduction process [53]. Moreover, trace quantity of nanostructures on the basal planes of rGO allows uniform dispersion of the nanocomposite in polar solvents, which is otherwise impossible for rGO [20].

4. A new class of graphene-based inorganic nanostructures

The morphological structure of graphene nanocomposites is varied and depends on the synthesis route. Ag/graphene was synthesized using a thermal expansion method and yielded uniformly distributed Ag nanoparticles on graphene sheets [25] (Figure 2a). Whereas the hydrothermal approach gave an assemble pyrite structured FeS_2 nanospheres [56] (Figure 2b), CuO nanospheres [59] (Figure 2c), TiO_2 nanoparticles [43] (Figure 2d) and ZnO nanoflowers [60] (Figures 2e and 2f). In the last example, some of the ZnO nanoflowers were brighter in the SEM image than others and seemed to be enveloped by a thin film of graphene. Since the functional groups, such as hydroxyl and epoxy groups, are attached to both sides of GO

sheets, the ZnO nanoflowers appear on both sides of the graphene support [61]. Another method based around microwave heating has been used to make SnO_2/graphene nanocomposite [19] (Figure 2g). At a higher magnification (Figure 2h), the SnO_2 nanoparticles were observed to uniformly adhere on the graphene sheets, with high density [19]. A simple, cost-effective, efficient, and green in situ deposition to synthesize Fe_3O_4 nanoparticles on graphene [20] (Figure 2i) has also been explored. The magnetic property of the Fe_3O_4/graphene nanocomposite allows the separation of composite from the solution by applying an external magnetic field (Figure 2j).

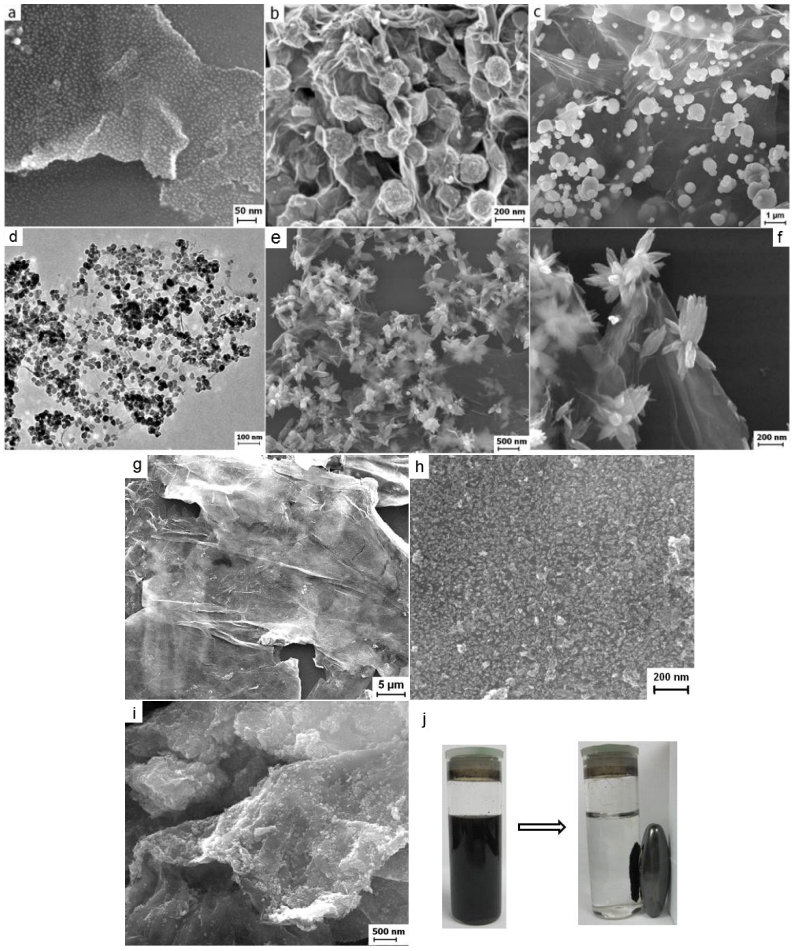

Figure 2. Electron micrographs of various inorganic nanostructures decorating graphene; (a) Ag, (b) FeS_2, (c) CuO, (d) TiO_2, (e) ZnO, (f) a higher magnification showing flower-like shape ZnO nanoarchitecture, (g) SnO_2, (h) a higher magnification revealing SnO_2 nanoparticles, and (i) Fe_3O_4. (j) Photo image of Fe_3O_4/graphene dispersed uniformly in water and attracted under the external magnetic field.

rGO has proven to be an effective matrix for the adhesion of nanostructures due to the rich content of oxide functional groups on the basal planes and edges of the 2-D material. Good evidence of rGO being an accomplished support is depicted through an FESEM image of Fe_3O_4/graphene, in which the nanocomposite was prepared at low concentration of Fe^{2+} ions. The micrograph of the sample shows no evidence for the formation of Fe_3O_4 nanoparticles (Figure 3a). This is in contrast to the sample prepared using a higher concentration of Fe^{2+} ions where nanoparticles are apparent (Figure 2i). To investigate this observation further, elemental mapping of C, O, and Fe using energy dispersive x-ray (EDX) analysis (Figure 3b) was undertaken (Figure 3c). The area of bright contrast correlates with the Fe signal map. This result, coupled with the XRD result [20], provides evidence for the presence of Fe_3O_4 on the surface of the graphene. The exact form of the Fe_3O_4 cannot be determined. It is possible that a layer of Fe_3O_4 has formed on the surface of the rGO or more likely that very small nanoparticles have formed.

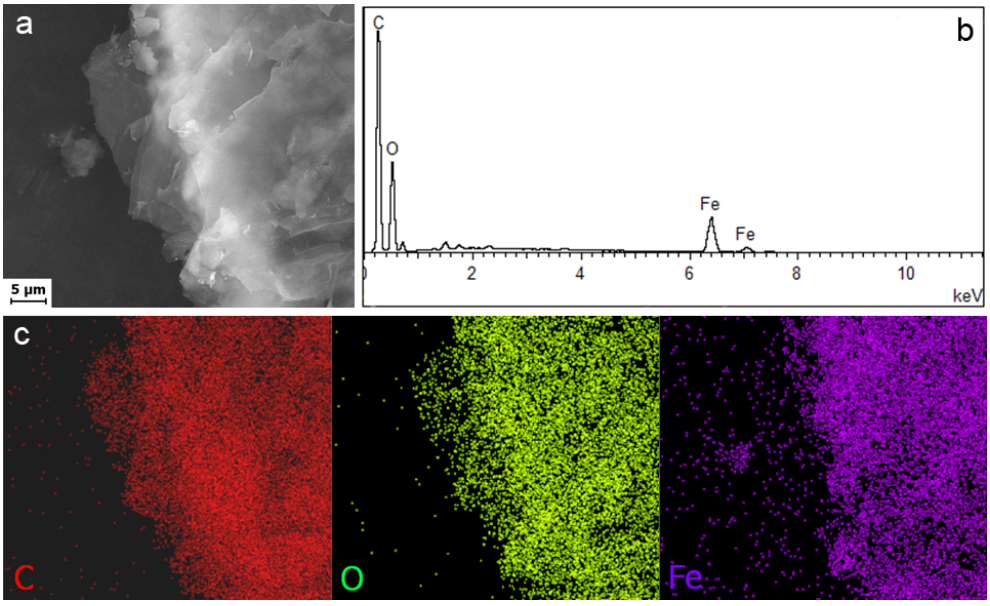

Figure 3. Fe_3O_4/graphene prepared at a low concentration of Fe^{2+} ions: (a) FESEM image, (b) EDX spectrum, and (c) elemental mapping [20].

5. Growth processes of inorganic nanostructures on graphene sheets

5.1. In situ chemical synthesis

In situ chemical synthesis is a robust route for the formation of graphene decorated with inorganic nanostructures. The attraction of the positively charged metal ions towards the

negatively charged electron cloud surrounding the oxygen atoms of the GO sheets is the initial step in the nucleation of the nanostructure on the graphene sheet. Since oxygen atoms are uniformly distributed in the starting graphene oxide sheets, a uniform decoration of nanostructures on the graphene sheets is produced after the reaction. Some metal oxides such as Fe_3O_4 and SnO_2 can grow on the surface of rGO at room temperature [20, 39]. However, by increasing the reaction temperature, the high temperature calcination step may be able to be eliminated e.g. SnO_2/graphene [42]. The reduction of GO may not occur during the deposition of the nanostructures on the surface of the GO, for example in the synthesis of MnO_2/GO [61]. To ensure the GO is completely reduced, additional reducing agents can be used. For example, in the synthesis of nanocrystal Ag/graphene, hydrazine and ammonia solution in the presence of polyvinyl alcohol were used [27].

In situ chemical synthesis has also been described as a one-pot thermodecomposition route. When graphene sheets are directly used, a stabilizing agent such as sodium dodecylbenzenesulfonate (SDBS) is required along with a high reaction temperature to encourage the assembly of the nanostructure. The formation of Fe nanostructures on graphene is an example of this. [54]. Similarly, CuO/graphene was synthesized through the stabilization of graphene sheet with ethylene glycol at a high temperature [34]. For some materials, however, the high reaction temperature is not required to promote the assembly. Ag_2O/graphene nanocomposites are an example and these were prepared in the presence of N-Methyl-2-pyrrolidone (NMP) under ambient conditions [33]. The stabilizing agents also function as a size- and shape-controlling agent and a reducing agent. In FeS_2/graphene, the stabilization agent constraints the growth of FeS_2 to a gelatin micelles geometry, resulting in well-formed nanoparticles [56]. Variations of the in situ chemical synthesis include the electrode-less Ni-plating on graphene sheets [29] and the attachment of Bi_2WO_6 nanoparticles and nanoplates onto GO by refluxing [49].

5.2. Hydrothermal

Hydrothermal synthesis is an efficient inorganic synthesis approach for the formation of a variety of nanomaterials, catalysts, ion-conductors, and zeolites [62] under controlled temperature and pressure. This synthesis route overcomes the drawbacks of high processing temperatures and long reaction times compared to conventional aqueous chemical processing conditions [63]. It has been recognized as an environmentally friendly process because the reaction uses aqueous solutions as a reaction medium and it is carried out in an autoclave, which is a closed system. This method can also be used for the preparation of high-purity, highly crystalline, ultrafine and homogeneous powders of various single and multi-component powders [64, 65]. The autoclave used in the hydrothermal synthesis, as mentioned previously, is a closed system and so raising its temperature increases the pressure inside the vessel above the critical pressure for water which enhances the dissolution of thermodynamically unstable compounds. The high heat energy and pressure in the autoclave facilitates fracture of the macronucleus to form nano-sized particles [66]. This method has been used for the synthesis of CuO/graphene [21], NiO/graphene [37], ZnO/graphene [47], and FeS_2/graphene nano-composites [56].

The hydrothermal systhesis methology is not restricted to pure aqueous solutions. The addition of other solvents like ethanol can be used to enhance the dispersion of gel-like GO [43]. For example, TiO_2 nanoparticles could be chemically bonded to the surface of rGO [45, 46]. Likewise, a one pot synthesis of Fe_2O_3 nanoparticles, Zn salt and GO produced Fe_2O_3-ZnO/graphene nanocomposites, in which the Fe_2O_3 nanoparticles were chemically bonded to the graphene sheets. The 50 nm sized Fe_2O_3 nanoparticles were covered with ZnO nanoparticles that are less than 10 nm in size [55].

If the solutions are not aqueous based, the method is known as the solvothermal process, for instance absolute ethanol was used as a medium for the synthesis of SnSb/graphene [57]. For the synthesis of CdS/graphene, dimethyl sulfoxide (DMSO) not only acted as a reaction medium but also the source of sulphide and a reducing agent [67]. SnO_2/graphene was prepared via a gas–liquid interfacial reaction, in a process similar to hydrothermal method. During the reaction, a two-phase liquid was vaporized, which allowed the Sn^{4+} to react with the ammonia at gas/liquid interface to produce $Sn(OH)_4$ along with in situ deposited onto the graphene sheets. The $Sn(OH)_4$ subsequently decomposed to SnO_2 on the graphene sheets [41]. Fe_3O_4/graphene has also been prepared using the same process [35].

5.3. Microwave heating

Microwave heating is believed to be more depending on the molecular properties and the reaction conditions than conventional heating [68]. Microwave syntheses have been increasingly used in the preparation of high monodispersity nanoparticles of oxides such as SnO_2, CeO_2 and ZrO_2 [69]. Utilizing microwave energy for the thermal treatment generally leads to very fine particles in the nanocrystalline regime mainly caused by the shorter synthesis time and a highly focused localised heating. The particle size often falls in the range of 15 nm – 35 nm [70]. Microwave heating also has been widely used for the fabrication of inorganic nanostructure/graphene where the particles were less than 10 nm with a narrow size distribution. In this synthesis, the graphene sheets obviously played an important role in constraining the growth of nanostructures [32, 71]. Hydrothermal method has also been combined with microwave heating to ensure a complete reduction of GO [40].

5.4. Electrodeposition

Electrodeposition provides a facile procedure and offers precise control of the thickness of the resulting film [72]. In addition to the speed of polymerization, which can be controlled by the current density [73], this method also enables mild processing conditions at room temperature [74], without toxic or excess chemicals [75]. GO is coated on the surface of a glassy carbon electrode (GCE) before being immersed into a salt solution. By cycling the potential, the metal salt is oxidized to metal oxide and the GO is reduced to graphene. This synthesis methodology has been used in the preparation of PbO/graphene [38] and ZrO_2/graphene [48].

Although it is known to be hydrophilic, GO does not peel off from the GCE surface when it is placed in aqueous electrolytes because of the interaction of hydrophobic regions of GCE and

the unoxidized portions of GO [38]. It does, however, swell in an aqueous solution as water molecules bond to the GO.

The formation of the actual graphene based GCE is problematic because it is difficult to obtain a uniform dispersion of graphene in a solvent. The graphene sheets when in solution tend to form irreversible agglomerates or even restack to graphite through strong π-π stacking and van der Waals interaction. If graphene is to be used for the modification of GCE, it must first be dispersed in a stabilizer to form a homogenous dispersion before being dropped cast on the GCE surface. The inorganic nanostructures on graphene are formed by cyclic voltammetry in the appropriate salt solution. An example of this method is the synthesis Ag/graphene [28].

Electrochemical co-deposition is another route to prepare inorganic nanostructure/graphene. Pd/graphene is an example, where a solution containing GO and a metal salt underwent voltammetry cycling simultaneously [30].

5.5. Other unusual strategic routes

There have been several novel processing routes that have been reported. A Ag precursor was physically grounded with dry GO before the product was heated at 1000°C for 20s to produce Ag/graphene [25]. This method produced high purity nanocomposite because the process did not require any reducing or stabilizing agents. The extreme condition spontaneously reduced the Ag ion to Ag metal, and GO to rGO. Inorganic nanostructure/graphene has also been prepared using irradiation (lasers [31], [26], and exposure to UV [50]). Layer-by-layer inorganic structure/graphene can be prepared by dipping-lifting in sol-gel solution [52]. Finally, ultrasonication of the starting solution was able to generate of Mn_3O_4/graphene nanocomposites [36].

6. Recent advances in the applications of inorganic nanostructure decorated graphene

6.1. Anode for lithium-ion batteries

Graphite-based lithium-ion batteries suffer from poor charge–discharge performance and consequently have poor power performance. In many applications like electric or hybrid cars, there will be periods of high power demand, for example accelerating to overtake a car, and this leads to increased heat dissipation in the cell and accelerated aging of the battery. The use of graphene electrodes significantly improves the power performance of the battery and has resulted in a significant number of papers. The versatility of graphene to accommodate lithium ions on both sides of its single atomic sheet provides high energy storage capacity above 600 $mAhg^{-1}$, which is higher than the theoretical capacity of graphite (372 $mAhg^{-1}$). Recently, the use of metal oxides and metal alloys graphene nanocomposite has improved the energy storage of graphene based electrodes even more (700–4000 $mAhg^{-1}$) [37]. The extra capacity has been attributed to the synergistic effect between the nanoparticles and graphene sheets in the nanocomposite, providing extra sites for the storage of lithium ions [35].

In any battery application, the degradation of the storage capacity with repeated charge-discharge cycles is extremely important. The cycling performance of graphene inorganic nanostructures far exceeds that of their individual counterparts [21, 35]. Moreover, graphene inorganic nanostructures also displayed excellent reversible specific capacities at a broad range of current densities [40-42]. The good lithium cycling performance is ascribed to the structural integrity of the composite electrodes. The nanocystals located on the surface of graphene prevented the agglomeration of graphene sheets. Likewise, the graphene sheets hindered the direct contact among the adjacent nanocrystals. Minimizing the aggregation of nanocrystals and graphene sheets during discharge/charge cycling gives rise to high surface area, excellent electronic conductivity of the electrodes by forming an efficient electrically conductive network, and high carrier mobility. This heterogeneous construction also provides buffering spaces against the volume changes of nanocrystals during the lithium insertion/extraction processes.

Regardless of the type of inorganic nanocrystal, the graphene nanocomposites have generally displayed a large irreversible capacity in the first cycle [51, 57]. It is widely reported that this phenomenon may be attributed to electrolyte decomposition and formation of solid electrolyte interface (SEI) film [76-78]. Irreversible capacity is the occurrence of naturally non-recoverable charge capacity, in which the kinetics will vary depending on the battery chemistry, electrode composition and design, electrolyte formulation and impurities, and on the storage temperature [79].

6.2. Supercapacitors

With the increase in affluence in developing countries, the energy needs are increasing and energy sustainability is of significant concern especially when the depletion of fossil fuels is also factored in [61]. Supercapacitors, also known as ultracapacitors or electrochemical supercapacitors, have several important characteristics, including prolonged life cycle [80, 81], higher power density than batteries [82] and higher energy density [83] than conventional capacitors which have driven their use in pulse power and power backup applications [84]. According to the mechanism of charge storage, supercapacitors can be classified as i) electric double layer capacitors (EDLCs) where charge is stored at the electrode/electrolyte interface, and ii) pseudocapacitors where the charge is stored mainly by Faradaic reactions on the surface of the electrode materials [85, 86].

Carbon-based materials are commonly used in EDLCs as electrodes because of its high electrical conductivity and outstanding long-term electrochemical stability as a result of the extraordinary chemical stability of carbon [87]. Carbon-based materials such as activated carbon [88], xerogels [89], carbon nanotubes [90], mesoporous carbon [91] and carbide-derived carbons [92] have all been investigated for use as electrodes in EDLC. However, the limited charge accumulation in electrical double layer restricts the specific capacitance of EDLCs to a relatively small range of values between 90 and 250 F/g [93]. Meanwhile, pseudocapacitors like metal oxides such as RuO_2 [94-96], NiO [96, 97], Co_3O_4 [98], MnO_2 [99], or conducting

polymers including polypyrole [100] and polyaniline [101, 102] usually show poor capacitance behavior.

Recently, graphene has been used as a supercapacitor electrode material due to its high surface area, excellent stability and good conductivity [103-106]. To effectively overcome the shortage of low specific capacitance, the 2-D structured graphene has been hybridized with pseudocapacitors for the preparation of supercapacitors [32, 107-109]. The specific capacitance and electrochemical stability of graphene inorganic structures is enhanced tremendously in comparison to their individual counterparts [33, 36]. The improvement of the supercapacitive behaviour is attributable to the different double-layer and pseudocapacitive contributions.

6.3. Photocatalysts

Organic effluents from industries, agricultural activities and the rapid increase in human waste as a result of the rapid population increase represents some of the most serious environmental pollutants. It is estimated that around four billion people worldwide have no or little access to clean and sanitized water supply, resulting in death, by severe waterborne diseases, of millions of people annually [110]. Photodegradation of organic pollutants has attracted increasing attention during the past decade as it appears to be a viable decontamination process with widespread application, regardless of the state (gas or liquid) or chemical nature of the process target [45, 111]. Photocatalytic oxidation is an economical process owing to the fact that it involves only a photocatalyst and light source [112]. This process does not yield toxic intermediate product, making it suitable for cleaning water environment that contains low to medium contaminants concentration [113].

When a photocatalyst is illuminated with the light of sufficient energy, electrons in the valence band of the photocatalyst are excited into the conduction band, therefore, creating the negative electron-positive hole pairs ($e^- - h^+$). When the photocatalyst is in contact with water, the $e^- - h^+$ pairs will initiate a series of reactions and produce hydroxyl radicals, $HO^\bullet$ and superoxide radical anions, $O^{\bullet +}$, on the photocatalyst surface. Any organic contaminants at or near to the photocatalyst surface are oxidized by the generated radicals [114, 115]. The most commonly used photocatalysts are titanium dioxide and zinc oxide, which are semiconductors. The drawback of these photocatalysts is the quick electron-hole recombination on the surface of semiconductors, which hampers the hydrogen evolution efficiency.

To manipulate the rate of electron-hole recombination, the presence of non-metal species like carbon, nitrogen, boron and fluorine are targeted to minimize photogenerated electron-hole recombination rate, thus improving quantum efficiency and expanding their useful range of operation into visible light wavelengths [116, 117]. Graphene, a uniform and thin transparent conducting material, is a potential carbon source.

Nanocrystals are not stable and prone to aggregate, which results in a reduced surface area and so limits the likelihood of the photoinduced electron–hole pairs interacting with water molecules to produce the radicals thereby decreasing the application efficiency. This can be overcome by using graphene as a supporting matrix for the photocatalyst particles, as well

as an electron acceptor, to improve the efficiency of the degradation of organic pollutants [67] and durability for consecutive photodegradation cycling [45, 49]. In addition, the giant π-conjugation of graphene and two-dimensional planar structure are the driving forces for the non-covalent adsorption between aromatic molecules and aromatic regions of the graphene [45].

Many photocatalysts have a wide band gap and so require UV light for operation. Since ultraviolet (UV) light accounts for only a small fraction (5%) of the Sun's energy as compared to visible light (45%); any shift in the optical response of a photocatalyst from the UV to the visible spectral range will have a profound positive effect on the photodegradation efficiency of a photocatalyst [118]. Incorporation of carbon is known to be able to reduce the band gap energy of a photocatalyst [116]. Photocatalysis using graphene inorganic structure could take place under the irradiation of visible light due to zero band semiconductor with symmetric K and K' [49].

On the other hand, the photoelectrocatalytic process takes advantage of the photocatalytic process by applying a biased voltage across a photo-electrode on which the photocatalysts are supported. An enhancement of the photocurrents using graphene nanocomposite electrodes is attributed to the enhanced migration efficiency of the photo-induced electrons and enhanced adsorption activity of the aromatic molecules [46]. Photoelectrocatalytic activity is dependent on the optimal value of graphene content, as superfluous graphene will reduce the absorption efficiency of light by a photocatalyst. Experiments have shown an increase in the degradation of the aromatic molecules by the graphene nanocomposite as the applied potential was increased relative to a reference electrode [119-124]. This was explained by the potential causing band bending close to the electrode surface reducing the potential barriers and improving the mobility of the carrier across the electrode, and hence minimizing the probability of recombination of electrons and holes and elevating the photoelectrocatalysis efficiency [124].

The overall excellent photocatalytic performance of graphene inorganic nanostructures is reportedly attributed to enhanced adsorptivity, extended light absorption range, efficient charge separation and transportation [45].

6.4. Sensing platform

Many analytical methods with high sensitivity and low detection limit have been established for determination of organic and inorganic matters [125]. However, they are time consuming, expensive, require complicated instruments and a skilled operator, which are unsuitable for on-line or in-field monitoring [126]. In contrast, electrochemical analysis, which has the advantages of quick response, cheap instrumentation, low power consumption, simplified operation, time-saving, high sensitivity and selectivity, is widely applied in applications such as gas sensing, chemical sensing and biosensing [27, 127-129].

Direct detection using bare electrode yields poor sensitivity to the target material [128]. Inorganic nanoparticles are versatile and sensitive tracers because of their high surface area,

high mechanical strength but ultra-light weight, rich electronic properties, and excellent chemical and thermal stability [130] and when coupled with graphene, they provided an attractive nanocomposite for the fabrication of electrochemical sensors [33, 131]. In this regard, inorganic nanostructure decorated graphene has been proven to be an effective tool to detect low amounts of biomarker [27], pesticide [48], heavy metals [28, 38, 39], and glucose [34], with high sensitivity, selectivity, stability and reproducibility.

6.5. Other interesting applications

Besides the four major applications stated above, graphene inorganic nanostructures have also been investigated for other purposes. These include direct formic acid fuel cells, which are widely considered to be one of the most attractive power sources [30]; providing a favourable catalytic pathway for the formation of CO_2 [31] to form CO [132]; and producing electrocatalytic activity for methanol oxidation [32]. Other uses of the structures is to produce a photocurrent under UV light or visible light illumination to meet the demand of renewable and clean energy source [52], assisting the conversion of solar energy into hydrogen via the water splitting process [133], and removing chromium(IV) in water through adsorption [54].

7. What does the future hold for inorganic nanostructure decorated graphene?

The significant potential of graphene-based inorganic nanostructure in solving many of today's problems is evident from the amount of effort that has been devoted to exploring the synthesis of the materials and the investigation of the materials in real-life applications. The cutting-edge research on graphene-based nanoinorganic materials has yet to mature. Drawing comparisons to silicone research, the interest will continue to grow until commercial products using graphene are realized. The simple and scalable production of GO, a derivative of graphene, that is rich in oxygenous functional groups, is encouragement for researchers to modify the surface of the one-atom thick carbon layers with a variety of inorganic nanostructures to cater for the commercial demands and needs. The quality of inorganic nanostructure decorated graphene at atomic level is assured by systematic characterization using state-of-the-art instruments. The graphene research offers novel and exciting opportunities for the scientific community and industrialists who seek new partnerships and advances.

Acknowledgements

This work was supported by the Exploratory Research Grant Scheme (ER016-2011A), High Impact Research Grants from the University of Malaya (UM.C/625/1/HIR/030) and High Impact Research Grants from the Ministry of Higher Education of Malaysia (UM.C/625/1/HIR/MOHE/05).

Author details

Hong Ngee Lim[1,2], Nay Ming Huang[3], Chin Hua Chia[4] and Ian Harrison[5]

1 Department of Chemistry, Faculty of Science, Universiti Putra Malaysia, UPM Serdang, Selangor, Malaysia

2 Functional Device Laboratory, Institute of Advanced Technology, Universiti Putra Malaysia, UPM Serdang, Selangor, Malaysia

3 Department of Physics, Faculty of Science, University of Malaya, Kuala Lumpur, Malaysia

4 School of Applied Physics, Faculty of Science and Technology, Universiti Kebangsaan Malaysia, Bangi, Selangor, Malaysia

5 Faculty of Engineering, The University of Nottingham Malaysia Campus, Jalan Broga, Semenyih, Selangor, Malaysia

References

[1] Chen, F, & Tao, N. J. Electron transport in single molecules: From benzene to graphene. Accounts of Chemical Research (2009). , 42(3), 429-38.

[2] Novoselov, K. S, Geim, A. K, Morozov, S. V, Jiang, D, Zhang, Y, Dubonos, S. V, Grigorieva, I. V, & Firsov, A. A. Electric field effect in atomically thin carbon films. Science (2004). , 306(5696), 666-9.

[3] Nair, R. R, Blake, P, Grigorenko, A. N, Novoselov, K. S, Booth, T. J, Stauber, T. Peres NMR, & Geim AK. Fine structure constant defines visual transparency of graphene. Science (2008). , 320(5881): 1308.

[4] Yu, A, Ramesh, P, Itkis, M. E, Bekyarova, E, & Haddon, R. C. Graphite nanoplatelet-epoxy composite thermal interface materials. Journal of Physical Chemistry C (2007). , 111(21), 7565-9.

[5] Pumera, M. The electrochemistry of carbon nanotubes: Fundamentals and applications. Chemistry- A European Journal (2009). , 15(20), 4970-8.

[6] Stoller, M. D, Park, S, Zhu, Y, An, J, & Ruoff, R. S. Graphene-based ultracapacitors. Nano Letters (2008). , 8(10), 3498-502.

[7] Bunch, J. S, Van Der Zande, A. M, Verbridge, S. S, Frank, I. W, Tanenbaum, D. M, Parpia, J. M, Craighead, H. G, & Mceuen, P. L. Electromechanical resonators from graphene sheets. Science (2007). , 315(5811), 490-3.

[8] Pumera, M. Electrochemistry of graphene: New horizons for sensing and energy storage. The Chemical Record (2009). , 9(4), 211-23.

[9] Chen, X. M, Wu, G. H, & Jiang, Y. Q. Wang YRC, X. Graphene and graphene-based nanomaterials: The promising materials for bright future of electroanalytical chemistry. Analyst (2011). , 136, 4631-40.

[10] Liang, R, Deng, M, Cui, S, Chen, H, & Qiu, J. Direct electrochemistry and electrocatalysis of myoglobin immobilized on zirconia/multi-walled carbon nanotube nanocomposite. Materials Research Bulletin (2010). , 45(12), 1855-60.

[11] Chiu, W. S, Khiew, P. S, Isa, D, Cloke, M, Radiman, S, Abd-shukor, R, Abdullah, M. H, & Huang, N. M. Synthesis of two-dimensional ZnO nanopellets by pyrolysis of zinc oleate. Chemical Engineering Journal (2008). , 142, 337-43.

[12] Huang, N. M, Radiman, S, Lim, H. N, Yeong, S. K, Khiew, P. S, Chiu, W. S, & Kong, S. N. Saeed GHM. Synthesis and characterization of ultra small PbS nanorods in sucrose ester microemulsion. Materials Letters (2009). , 63, 500-3.

[13] Huang, N. M, Radiman, S, Lim, H. N, Yeong, S. K, Khiew, P. S, & Chiu, W. S. Saeed GHM, Nadarajah K. Gamma-ray assisted synthesis of Ni_3Se_2 nanoparticles stabilized by natural polymer. Chemical Engineering Journal (2009). , 147, 399-404.

[14] Chiu, W. S, Khiew, P. S, Cloke, M, Isa, D, Lim, H. N, Tan, T. K, Huang, N. M, Radiman, S, & Abd-shukor, R. Hamid MAA, Chia CH. Heterogeneous seeded growth: Synthesis and characterization of bifunctional Fe_3O_4/ZnO core/shell nanocrystals. The Journal of Physical Chemistry C (2010). , 114(18), 8212-8.

[15] Zhou, X, Huang, X, Qi, X, Wu, S, & Xue, C. Boey FYC, Yan Q, Chen P, Zhang H. In situ synthesis of metal nanoparticles on single-layer graphene oxide and reduced graphene oxide surfaces. The Journal of Physical Chemistry C (2009). , 113(25), 10842-6.

[16] Alivisatos, A. P. Semiconductor clusters, nanocrystals, and quantum dots. Science (1996). , 271(5251), 933-7.

[17] Geim, A. K. Graphene: Status and prospects. Science (2009). , 324(5934), 1530-4.

[18] Geim, A. K, & Novoselov, K. S. The rise of graphene. Nature Materials (2007). , 6(3), 183-91.

[19] Lim, H. N, Nurzulaikha, R, Harrison, I, Lim, S. S, Tan, W. T, Yeo, M. C, Yarmo, M. A, & Huang, N. M. Preparation and characterization of tin oxide, SnO_2 nanoparticles decorated graphene. Ceramics International (2012). , 38(5), 4209-16.

[20] Teo, P. S, Lim, H. N, Huang, N. M, Chia, C. H, & Harrison, I. Room temperature in situ chemical synthesis of Fe_3O_4/graphene. Ceramics International (2012). , 38, 6411-6.

[21] Mai, Y. J, Wang, X. L, Xiang, J. Y, Qiao, Y. Q, Zhang, D, Gu, C. D, & Tu, J. P. CuO/graphene composite as anode materials for lithium-ion batteries. Electrochimica Acta (2011). , 56(5), 2306-11.

[22] Singh, V, Joung, D, Zhai, L, Das, S, Khondaker, S. I, & Seal, S. Graphene based materials: Past, present and future. Progress in Materials Science (2011). , 56, 1178-271.

[23] Bai, S, & Shen, X. Graphene-inorganic nanocomposites. RSC Advances (2012). , 2, 64-98.

[24] Huang, N. M, Lim, H. N, Chia, C. H, Yarmo, M. A, & Muhamad, M. R. Simple room-temperature preparation of high-yield large-area graphene oxide. International Journal of Nanomedicine (2011). , 6, 3443-8.

[25] Zainy, M, & Huang, N. M. Vijay Kumar S, Lim HN. Simple and scalable preparation of reduced graphene oxide-silver nanocomposite via rapid thermal treatment. Materials Letters (2012). , 89, 180-3.

[26] Moussa, S, Atkinson, G, Shall, M. S, & Shehata, A. AbouZeid KM, Mohamed MB. Laser assisted photocatalytic reduction of metal ions by graphene oxide. Journal of Materials Chemistry (2011). , 21, 9608-19.

[27] Su, B, Tang, D, Li, Q, Tang, J, & Chen, G. Gold-silver-graphene hybrid nanosheets-based sensors for sensitive amperometric immunoassay of alpha-fetoprotein using nanogold-enclosed titania nanoparticles as labels. Analytica Chimica Acta (2011). , 692, 116-24.

[28] Gong, J, Zhou, T, Song, D, & Zhang, L. Monodispersed Au nanoparticles decorated graphene as an enhanced sensing platform for ultrasensitive stripping voltammetric detection of mercury(II). Sensors and Actuators B: Chemical (2010). , 150, 491-7.

[29] Hu, Q. H, Wang, X. T, Chen, H, & Wang, Z. Synthesis of Ni/graphene sheets by an electroless Ni-plating method. New Carbon Materials (2012). , 27(1), 35-41.

[30] Jiang, Y. Y, Lu, Y. Z, Li, F. H, Wu, T. S, Niu, L, & Chen, W. Facile electrochemical codeposition of “clean” graphene-Pd nanocomposite as an anode catalyst for formic acid electrooxidation. Electrochemistry Communications (2012). , 19, 21-4.

[31] Moussa, S, Abdelsayed, V, & Shall, M. S. Laser synthesis of Pt, Pd, CoO and Pd-CoO nanoparticle catalysts supported on graphene. Chemical Physics Letters (2011).

[32] Wang, S, Jiang, S. P, & Wang, X. Microwave-assisted one-pot synthesis of metal/metal oxide nanoparticles on graphene and their electrochemical applications. Electrochimica Acta (2011). , 56(9), 3338-44.

[33] Chen, S, Zhu, J, & Wang, X. An in situ oxidation route to fabricate graphene nanoplate-metal oxide composites. Journal of Solid State Chemistry (2011). , 184(6), 1393-9.

[34] Hsu, Y. W, Hsu, T. K, Sun, C. L, Nien, Y. T, Pu, N. W, & Ger, M. D. Synthesis of CuO/graphene nanocomposites for nonenzymatic electrochemical glucose biosensor applications. Electrochimica Acta (2012). , 82, 152-7.

[35] Lian, P, Zhu, X, Xiang, H, Li, Z, Yang, W, & Wang, H. Enhanced cycling performance of Fe_3O_4-graphene nanocomposite as an anode material for lithium-ion batteries. Electrochimica Acta (2010). , 56(2), 834-40.

[36] Wang, B, Park, J, Wang, C, Ahn, H, Wang, G, & Mn, O. nanoparticles embedded into graphene nanosheets: Preparation, characterization, and electrochemical properties for supercapacitors. Electrochimica Acta (2011). , 55(22), 6812-7.

[37] Kottegoda IRM, Idris NH, Lu L, Wang JZ, Liu HK. Synthesis and characterization of graphene-nickel oxide nanostructures for fast charge-discharge application. Electrochimica Acta (2011). , 56(16), 5815-22.

[38] Ramesha, G. K, & Sampath, S. In-situ formation of graphene-lead oxide composite and its use in trace arsenic detection. Sensors and Actuators B: Chemical (2011). , 160, 306-11.

[39] Wei, Y, Gao, C, Meng, FL, Li, HH, Wang, L, Liu, JH, & Huang, XJ. SnO_2/reduced graphene oxide nanocomposite for the simultaneous electrochemical detection of cadmium(II), lead(II), copper(II), and mercury(II): An interesting favorable mutual interference. Journal of Physical Chemistry C 2011;116: 1034-41.

[40] Zhong, C, Wang, J, Chen, Z, & Liu, H. SnO_2-graphene composite synthesized via an ultrafast and environmentally friendly microwave autoclave method and its use as a superior anode for lithium-ion batteries. The Journal of Physical Chemistry C 2011;115: 25115-20.

[41] Lian, P, Zhu, X, Liang, S, Li, Z, Yang, W, & Wang, H. High reversible capacity of SnO_2/graphene nanocomposite as an anode material for lithium-ion batteries. Electrochimica Acta (2011). , 56(12), 4532-9.

[42] Yao, J, Shen, X, Wang, B, Liu, H, & Wang, G. In situ chemical synthesis of SnO_2-graphene nanocomposite as anode materials for lithium-ion batteries. Electrochemistry Communications (2009). , 11(10), 1849-52.

[43] Chang BYS, Huang NM, An'amt MN, Marlinda AR, Norazriena Y, Muhamad MR, Harrison I, Lim HN, Chia CH.Facile hydrothermal preparation of titanium dioxide decorated reduced graphene oxide nanocomposite. International Journal of Nanomedicine (2012). , 7, 3379-87.

[44] Guo, J, Zhu, S, Chen, Z, Li, Y, Yu, Z, Liu, Q, Li, J, Feng, C, & Zhang, D. Sonochemical synthesis of TiO_2 nanoparticles on graphene for use as photocatalyst. Ultrasonics Sonochemistry (2011). , 18(5), 1082-90.

[45] Zhang, H, Lv, X, Li, Y, Wang, Y, & Li, J. P25-graphene composite as a high performance photocatalyst. ACS Nano (2010). , 4(1), 380-6.

[46] Wang, P, Ao, Y, Wang, C, Hou, J, & Qian, J. Enhanced photoelectrocatalytic activity for dye degradation by graphene-titania composite film electrodes. Journal of Hazardous Materials (2012).

[47] Marlinda, A. R, Huang, N. M, & Muhamad, M. R. An'amt MN, Chang BYS, Yusoff N, Harrison I, Lim HN, Vijay Kumar S. Highly efficient preparation of ZnO nanorods decorated reduced graphene oxide nanocomposites. Materials Letters (2012). , 80, 9-12.

[48] Gong, J, Miao, X, Wan, H, & Song, D. Facile synthesis of zirconia nanoparticles-decorated graphene hybrid nanosheets for an enzymeless methyl parathion sensor. Sensors and Actuators B: Chemical (2012). , 162, 341-7.

[49] Min, Y. L, Zhang, K, Chen, Y. C, & Zhang, Y. G. Enhanced photocatalytic performance of Bi_2WO_6 by graphene supporter as charge transfer channel. Separation and Purification Technology (2012). , 86, 98-105.

[50] Wu, C. H, Zhang, Y. Z, Li, S, Zheng, H. J, Wang, H, Liu, J. B, Li, K. W, & Yan, H. Synthesis and photocatalytic properties of the graphene-$La_2Ti_2O_7$ nanocomposites. Chemical Engineering Journal (2011). , 178, 468-74.

[51] Fu, Y, Wan, Y, Xia, H, & Wang, X. Nickel ferrite-graphene heteroarchitectures: Toward high-performance anode materials for lithium-ion batteries. Journal of Power Sources (2012). , 213, 338-42.

[52] Li, G, Wang, T, Zhua, Y, Zhang, S, Mao, C, Wu, J, Jin, B, & Tian, Y. Preparation and photoelectrochemical performance of Ag/graphene/TiO_2 composite film. Aplied Surface Science (2011). , 257, 6568-72.

[53] Wang, X, Tian, X, H, Yang, H, Y, Wang, Y, H, Wang, H, S, Zhang, S, W, & Liu, W, Y. Y. Reduced graphene oxide/CdS for efficiently photocatalystic degradation of methylene blue. Journal of Alloys and Compounds (2012). , 524, 5-12.

[54] Zhu, J, Wei, S, Gu, H, Rapole, S. B, Wang, Q, Luo, Z, Haldolaarachchige, N, Young, D. P, & Guo, Z. One-pot synthesis of magnetic graphene nanocomposites decorated with core@double-shell nanoparticles for fast chromium removal. Environmental Science and Technology (2012). , 46, 977-85.

[55] Vijay Kumar, S, Huang, NM, Yusoff, N, Lim, HN. High performance magnetically separable graphene/zinc oxide nanocomposite. Materials Letters (2012). , 93, 411-4.

[56] Golsheikh, A. M, Huang, N. M, Lim, H. N, Chia, C. H, Harrison, I, & Muhamad, M. R. One-pot hydrothermal synthesis and characterization of FeS_2 (pyrite)/graphene nanocomposite. Chemical Engineering Journal (2012). DOI:http://dx.doi.org/10.1016/j.cej.2012.09.082.

[57] Xie, J, Song, W, Zheng, Y, Liu, S, Zhu, T, Cao, G, & Zhao, X. Preparation and Li-storage properties of SnSb/graphene hybrid nanostructure by a facile one-step solvothermal route. International Journal of Smart and Nano Materials (2011). , 2(4), 261-71.

[58] Xue, Y, Chen, H, Yu, D, Wang, S, Yardeni, M, Dai, Q, Guo, M, Liu, Y, Lu, F, Qu, J, & Dai, L. Oxidizing metal ions with graphene oxide: The in situ formation of magnetic nanoparticles on self-reduced graphene sheets for multifunctional applications. Chemical Communication (2011). , 47, 1689-91.

[59] Yusoff, N, Huang, NM, Muhamad, MR, Kumar, SV, Lim, HN, Harrison, I. Hydrothermal synthesis of copper oxide/functionalized graphene nanocomposites for dye degradation. Materials Letters (2012). , 93: 393-6.

[60] Huang, N. M, Marlinda, A. R, & Lim, H. N. inventors; Efficient fabrication of flower-like ZnO/reduced functionalized graphene oxide nanocomposites for gas sensing applications. Patent filed. (2012).

[61] Chen, S, Zhu, J, Wu, X, Han, Q, & Wang, X. Graphene oxide-MnO_2 nanocomposites for supercapacitors. ACS Nano (2010). , 4(5), 2822-930.

[62] Lim, H. N, Kassim, A, & Lim, S. P. RastamNizar NS, Huang NM. Microstructural changes of carbonaceous monoliths synthesized via hydrothermal. Journal of the Chilean Chemical Society (2011). , 56(1), 584-6.

[63] Zakarya, S. A, Kassim, A, Lim, H. N, Anwar, N. S, & Huang, N. M. Synthesis of titanium dioxide microstructures via sucrose ester microemulsion-mediated hydrothermal method. Sains Malaysiana (2010). , 39(6), 975-9.

[64] Anwar, N. S, Kassim, A, Lim, H. N, Zakarya, S. A, & Huang, N. M. Synthesis of titanium dioxide nanoparticles via sucrose ester micelle-mediated hydrothermal processing route. Sains Malaysiana (2010). , 39(2), 261-5.

[65] Lim, H. N, Kassim, A, & Huang, N. M. Preparation and characterization of calcium phosphate nanorods using reverse microemulsion and hydrothermal processing routes. Sains Malaysiana (2010). , 39(2), 267-73.

[66] Haw, C. Y, Mohamed, F, Radiman, S, Chia, C. H, Huang, N. M, & Lim, H. N. Hydrothermal synthesis of magnetite nanoparticles as MRI contrast agents. Ceramics International (2010). , 36(4), 1417-22.

[67] Wang, X, Tian, H, Yang, Y, Wang, H, Wang, S, Zhang, W, & Liu, Y. Reduced graphene oxide/CdS for efficiently photocatalystic degradation of methylene blue. Journal of Alloys and Compounds (2012). , 524, 5-12.

[68] Dressen, M. Microwave heating in fine chemical applications: Role of heterogeneity. Thesis (2009).

[69] Wang, Y, & Lee, J. Y. Microwave-assisted synthesis of SnO_2-graphite nanocomposites for Li-ion battery applications. Journal of Power Sources (2005). , 144, 220-5.

[70] Subramanian, V, Burke, W. W, Zhu, H, & Wei, B. Novel microwave synthesis of nanocrystalline SnO_2 and its electrochemical properties. Journal of Physical Chemistry C (2008). , 112, 4550-6.

[71] Zhang, M, Lei D, Du Z, Yin X, Chen L, Li Q, Wang Y, Wang T. Fast synthesis of SnO_2/graphene composites by reducing graphene oxide with stannous ions. Journal of Materials Chemistry (2010). , 21, 1673-6.

[72] Tully, E, Higson, S. P, & Kennedy, O. R. The development of a'labeless' immunosensor for the detection of Listeria monocytogenes cell surface protein, Internalin B. Biosensors and Bioelectronics (2008). , 23, 906-12.

[73] Zhang, J, Kong, L, Wang, B, Luo, Y, & Kang, L. In-situ electrochemical polymerization of multi-walled carbon nanotube/polyaniline composite films for electrochemical supercapacitors. Synthetic Metals (2009). , 159, 260-6.

[74] Torres, S, Neculqueo, G, & Martinez, F. Morphological and structural characterization of poly(3-decylthiophene) prepared by electropolymerization using 1-butyl-3-methyl-imidazoliumtetrafluorborate as solvent. Journal of the Chilean Chemical Society (2007). , 52(3), 1235-6.

[75] Tsai, M, Chen, P, & Do, J. Preparation and characterization of Ppy/Al_2O_3/Al used as a solid state capacitor. Journal of Power Sources (2004). , 133, 302-11.

[76] Li, Y, Lv, X, Lu, J, & Li, J. Preparation of SnO_2-nanocrystal/graphene-nanosheets composites and their lithium storage ability. Journal of Physical Chemistry C (2010). , 114, 21770-4.

[77] He, Y, Huang, L, Cai, J. S, Zheng, X. M, & Sun, S. G. Structure and electrochemical performance of nanostructured Fe_3O_4/carbon nanotube composites as anodes for lithium ion batteries. Electrochimica Acta (2010). , 55, 1140-4.

[78] Muraliganth, T, Murugan, A. V, & Manthiram, A. Facile synthesis of carbon-decorated single-crystalline Fe_3O_4 nanowires and their application as high performance anode in lithium ion batteries. Chemical Communication (2009). , 47, 7360-2.

[79] Yazami, R, & Reynier, Y. F. Mechanism of self-discharge in graphite-lithium anode. Electrochimica Acta (2002). , 47, 1217-23.

[80] Ran, L. Seung lC, Sang BL. Poly(3,4ethylenedioxythiophene) nanotubes as electrode materials for a high-powered supercapacitor. Nanotechnology (2008). pp).

[81] Ruiz, V, Blanco, C, Granda, M, & Santamaria, R. Enhanced life-cycle supercapacitors by thermal treatment of mesophase-derived activated carbons. Electrochimica Acta (2008). , 54, 305-10.

[82] Portet, C, Taberna, P. L, Simon, P, Flahaut, E, & Laberty-robert, C. High power density electrodes for carbon supercapacitor applications. Electrochimica Acta (2005). , 50, 4174-81.

[83] Hu, X, Deng, Z, Suo, J, & Pan, Z. A high rate, high capacity and long life ($LiMn_2O_4$ + AC)/$Li_4Ti_5O_{12}$ hybrid battery-supercapacitor. Journal of Power Sources (2009). , 187, 635-9.

[84] Jayalakshmi, M, & Balasubramaniam, K. Simple capacitors to supercapacitors- An overview. International Journal of Electrochemistry (2008). , 3, 1196-217.

[85] Simon, P, & Gogotsi, Y. Materials for electrochemical capacitors. Nature Materials (2008). , 7, 845-54.

[86] Lang, X, Hirata, A, Fujita, T, & Chen, M. Nanoporous metal/oxide hybrid electrodes for electrochemical supercapacitors. Nature Nanotechnology (2011). , 6, 232-6.

[87] Li, Q, Li, Z, Lin, L, Wang, X. Y, Wang, Y, Zhang, C, & Wang, H. Facile synthesis of activated carbon/carbon nanotubes compound for supercapacitor application. Chemical Engineering Journal (2010). , 156, 500-4.

[88] Frackowiak, E, & Beguin, F. Carbon materials for the electrochemical storage of energy in capacitors. Carbon (2001). , 39, 937-50.

[89] Mayer, S. T, Perkala, R. W, & Kaschmitter, J. L. The aerocapacitor: An electrochemical double-layer energy-storage device. Journal of the Electrochemical Society (1993). , 140(2), 446-51.

[90] Kaempgen, M, Chan, C. K, Ma, J, Cui, Y, & Gruner, G. Printable thin film supercapacitors using single-walled carbon nanotubes. Nano Letters (2009). , 9, 1872-6.

[91] Prabaharan SRS, Vimala R, Zainal Z.Nanostructured mesoporous carbon as electrodes for supercapacitors. Journal Power Sources (2006). , 161, 730-6.

[92] Chmiola, J, Yushin, G, Dash, R, & Gogotsi, Y. Effect of pore size and surface area of carbide derived carbons on specific capacitance. Journal Power Sources (2006). , 158, 765-72.

[93] Lu, X, Wang, G, Zhai, T, Yu, M, Gan, J, Tong, Y, & Li, Y. Hydrogenated TiO_2 nanotube arrays for supercapacitors. Nano Letters (2012). , 12, 1690-6.

[94] Wu, Z, Wang, D, Ren, W, Zhao, J, Zhou, G, Li, F, & Cheng, H. Anchoring hydrous RuO_2 on graphene sheets for high-performance electrochemical capacitors. Advanced Functional Materials (2010). , 20, 3595-602.

[95] Wang, H, Robinson, J. T, Li, X, & Dai, H. Solvothermal reduction of chemically exfoliated graphene sheets. Journal of the American Chemical Society (2009). , 131, 9910-1.

[96] Wang, H, Liang, Y, Mirfakhrai, T, Chen, Z, Casalongue, H, & Dai, H. Advanced asymmetrical supercapacitors based on graphene hybrid materials. Nano Research (2011). , 4, 729-36.

[97] Zhao, B, Song, J, Liu, P, Xu, W, Fang, T, Jiao, Z, Zhang, H, & Jiang, Y. Monolayer graphene/NiO nanosheets with two-dimension structure for supercapacitors. Journal of Materials Chemistry (2011). , 21, 18792-8.

[98] Zhou, W, Liu, J, Chen, T, Tan, K. S, Jia, X, Luo, Z, Cong, C, Yang, H, Li, C. M, & Yu, T. Fabrication of Co_3O_4-reduced graphene oxide scrolls for high-performance supercapacitor electrodes. Physical Chemistry Chemical Physics (2011). , 13, 14462-5.

[99] Cheng, Q, Tang, J, Ma, J, Zhang, H, Shinya, N, & Qin, L. Graphene and nanostructured MnO_2 composite electrodes for supercapacitors. Carbon (2011). , 49, 2917-25.

[100] Si, P, Ding, S, Lou, X, & Kim, D. An electrochemically formed three-dimensional structure of polypyrrole/graphene nanoplatelets for high-performance supercapacitors. RSC Advances (2011). , 1, 1271-127.

[101] Zhang, K, Zhang, L. L, Zhao, X. S, & Wu, J. Graphene/polyaniline nanofiber composites as supercapacitor electrodes. Chemistry of Materials (2010). , 22, 1392-401.

[102] Wang, H, Hao, Q, Yang, X, Lu, L, & Wang, X. A nanostructured graphene/polyaniline hybrid material for supercapacitors. Nanoscale (2010). , 2, 2164-70.

[103] Wang, Y, Shi, Z, Huang, Y, Ma, Y, Wang, C, Chen, M, & Chen, Y. Supercapacitor devices based on graphene materials. Journal of Physical Chemistry C (2009). , 113, 13103-7.

[104] Liu, C, Yu, Z, Neff, D, Zhamu, A, & Jang, B. Z. Graphene-based supercapacitor with an ultrahigh energy density. Nano Letters (2010). , 10, 4863-8.

[105] Kim, T. Y, Lee, H. W, Stoller, M, Dreyer, D. R, Bielawski, C. W, Ruoff, R. S, & Suh, K. S. High-performance supercapacitors based on poly(ionic liquid)-modified graphene electrodes. ACS Nano (2011). , 5, 436-42.

[106] Stoller, M. D, Park, S, Zhu, Y, An, J, & Ruoff, R. S. Graphene-based ultracapacitors. Nano Letters (2008). , 8, 3498-502.

[107] Dong, X, Xu, H, Wang, X, Huang, Y, Chan-park, M, Zhang, H, Wang, L, Huang, W, & Chen, P. 3D Graphene-cobalt oxide electrode for high-performance supercapacitor and enzymeless glucose detection. ACS Nano (2012). , 6, 3206-13.

[108] Rakhi, R. B, Chen, W, Cha, D, & Alshareef, H. N. High performance supercapacitors using metal oxide anchored graphene nanosheet electrodes. Journal of Materials Chemistry (2011). , 21, 16197-204.

[109] Su, H, Wang, T, Zhang, S, Song, J, Mao, C, Niu, H, Jin, B, Wu, J, & Tian, Y. Facile synthesis of polyaniline/TiO_2/graphene oxide composite for high performance supercapacitors. Solid State Sciences (2012). , 14, 677-81.

[110] Chong, M. N, & Jin, B. Chow CWK, Saint C. Recent developments in photocatalytic water treatment technology: A review. Water Research (2010). , 44(10), 2997-3027.

[111] He, Y, Wu, Y, Guo, H, Sheng, T, & Wu, X. Visible light photodegradation of organics over VYO composite catalyst. Journal of Hazardous Materials (2009). , 169, 855-60.

[112] Jiang, R, Zhu, H, Li, X, & Xiao, L. Visible light photocatalytic decolourization of C. I. Acid Red 66 by chitosan capped CdS composite nanoparticles. Chemical Engineering Journal (2009). , 152, 537-42.

[113] Fatin, S. O, Lim, H. N, Tan, W. T, & Huang, N. M. Comparison of photocatalytic activity and cyclic voltammetry of zinc oxide and titanium dioxide nanoparticles toward degradation of methylene blue. International Journal of Electrochemical Science (2012). , 7, 9074-84.

[114] Kropp, R, Tompkins, D, Barry, T, Zeltner, W, Pepping, G, Anderson, M, & Barry, T. A device that converts aqueous ammonia into nitrogen gas. Aquacultural Engineering (2009). , 41(1), 28-34.

[115] Soltaninezhad, M, & Aminifar, A. A. Study nanostructures of semiconductor zinc oxide (ZnO) as a photocatalyst for the degradation of organic pollutants. International Journal of Nanodimension (2011). , 2, 137-45.

[116] Im, J. S, Yun, S. M, & Lee, Y. S. Investigation of multielemental catalysts based on decreasing the band gap of titania for enhanced visible light photocatalysis. Journal of Colloid and Interface Science (2009). , 336, 183-8.

[117] Georgieva, J, Armyanov, S, Poulios, I, & Sotiropoulos, S. An all-solid photoelectrochemical cell for the photooxidation of organic vapours under ultraviolet and visible light illumination. Electrochemistry Communications (2009). , 11(8), 1643-6.

[118] Zhang, X, Jing, D, & Guo, L. Effects of anions on the photocatalytic H_2 production performance of hydrothermally synthesized Ni-doped $Cd_{0.1}Zn_{0.9}S$ photocatalysts. International Journal of Hydrogen Energy (2010). , 35(13), 7051-7.

[119] Tryk, D. A, Fujishima, A, & Honda, K. Recent topics in photoelectrochemistry: Achievements and future prospects. Electrochimica Acta (2000). , 45, 2363-76.

[120] Waldner, G, & Krysa, J. Photocurrents and degradation rates on particulate TiO_2 layers: Effect of layer thickness, concentration of oxidizable substance and illumination direction. Electrochimica Acta (2005). , 50, 4498-504.

[121] Carneiro, P. A, Osugi, M. E, Sene, J. J, & Anderson, M. A. Zanoni MVB. Evaluation of color removal and degradation of a reactive textile azo dye on nanoporous TiO2 thin film electrodes. Electrochimica Acta (2004). , 49(22-23), 3807-20.

[122] Solarska, R, Rutkowska, I, Morand, R, & Augustynski, J. Photoanodic reactions occurring at nanostructured titanium dioxide films. Electrochimica Acta (2006). , 51(11), 2230-6.

[123] Hepel, M, & Hazelton, S. Photoelectrocatalytic degradation of diazo dyes on nanostructured WO3 electrodes. Electrochimica Acta (2005).50(25-26): 5278-91.

[124] Hepel, M, & Hazelton, S. Photoelectrocatalytic degradation of diazo dyes on nanostructured WO_3 electrodes. Electrochimica Acta (2005). , 50(25-26): 5278-91.

[125] Ballesteros-gómez, A, Rubio, S, & Pérez-bendito, D. Analytical methods for the determination of bisphenol A in food. Journal of Chromatography A (2009). , 1216(3), 449-69.

[126] Yin, H, Cui, L, Chen, Q, Shi, W, Ai, S, Zhu, L, & Lu, L. Amperometric determination of bisphenol A in milk using PAMAM-Fe_3O_4 modified glassy carbon electrode. Food Chemistry (2011). , 125(3), 1097-103.

[127] Lim, H. N, Nurzulaikha, R, Harrison, I, Lim, S. S, Tan, W. T, & Yeo, M. C. Spherical tin oxide, SnO_2 particles fabricated via facile hydrothermal method for detection of mercury (II) ions. International Journal of Electrochemical Science (2011). , 6, 4329-40.

[128] Wang, F, Yang, J, & Wu, K. Mesoporous silica-based electrochemical sensor for sensitive determination of environmental hormone bisphenol A. Analytica Chimica Acta (2009). , 638(1), 23-8.

[129] Matin, B. M, Mortazavi, Y, Khodadadi, A. A, Abbasi, A, & Firooz, A. A. Alkaline- and template-free hydrothermal synthesis of stable SnO_2 nanoparticles and nanorods for CO and ethanol gas sensing. Sensors and Actuators B: Chemicals (2010). , 151, 140-5.

[130] Siangproh, W, Dungchai, W, Rattanarat, P, & Chailapakul, O. Nanoparticle-based electrochemical detection in conventional and miniaturized systems and their bioanalytical applications: A review. Analytica Chimica Acta (2011). , 690, 10-25.

[131] Yang, M, Javadi, A, & Gong, S. Sensitive electrochemical immunosensor for the detection of cancer biomarker using quantum dot functionalized graphene sheets as labels. Sensors and Actuators B: Chemical (2011). , 155, 357-60.

[132] Ligthart DAJM, van Santen RA & Hensen EJM. Supported rhodium oxide nanoparticles as highly active CO oxidation catalysts. Angewandte Chemie International Edition (2011). , 50, 5306-10.

[133] Biswal, N, Das, D. P, Martha, S, & Parida, K. M. Efficient hydrogen production by composite photocatalyst CdS-ZnS/zirconium-titanium phosphate (ZTP) under visible light illumination. International Journal of Hydrogen Energy (2011). , 36, 13452-60.